

# Simulation Study on neutrino nucleus cross section measurement in Segmented Detector at Spallation Neutron Source<sup>\*</sup>

YANG Zhen-wei<sup>1,2,3,1)</sup> DING Ming-ming<sup>1,2,3</sup> CHEN Shao-min<sup>1,2,3</sup>  
WANG Zhe<sup>3</sup> ZHANG Feng<sup>1,2,3</sup> GAO Yuan-ning<sup>1,2,3</sup>

<sup>1</sup> Key Laboratory of Particle & Radiation Imaging (Tsinghua University), Ministry of Education

<sup>2</sup> Department of Engineering Physics, Tsinghua University, Beijing 100084, P. R. China

<sup>3</sup> Center for High Energy Physics, Tsinghua University, Beijing 100084, P. R. China

**Abstract:** Knowledge of  $\nu_e$ -Fe/Pb differential cross sections for  $\nu_e$  energy below several tens of MeV scale is believed to be crucial in understanding Supernova physics. In a segmented detector at Spallation Neutrino Source,  $\nu_e$  energy reconstructed from the electron range measurement is strongly affected because of both multiple scattering and electromagnetic showers occurring along the electron passage in target materials. In order to estimate the effect, a simulation study has been performed with a cube block model assuming a perfect tracking precision. The distortion of energy spectrum is observed to be proportional to the atomic number of target material. Feasibility of unfolding the distorted  $\nu_e$  energy spectrum is studied for both Fe and Pb cases. Evaluation of statistical accuracy attainable is therefore provided for a segmented detector.

**Key words:** unfolding, neutrino, differential cross section, segmented detector, Monte Carlo, SNS, supernova

**PACS:** 29.30.Dn, 29.40.Wk, 95.55.Vj

## 1 Introduction

Precise knowledge of the differential cross sections for quasi-elastic neutrino-nucleus scattering at a scale up to several tens of MeV is of importance in understanding the explosion dynamics of supernova, since the neutrinos play a decisive role in the development between the prompt shock and the delayed shock [1]. Among the cross sections neutrino interactions with  $^2\text{H}$ , C, O, Fe and Pb are most relevant. In this low energy scale, the cross section varies rapidly, leading to large uncertainty in predicting the core collapse supernova [2, 3]. Although some theoretical calculations [4] of neutrino-nucleus cross sections have been performed in recent years, large uncertainties still exist and need to be clarified from experiments. On the experiment side, the differential cross sections with C and O have been measured by KARMEN and LSND experiments [5, 6], but those with Fe and Pb are still not available. In this paper, we present a simulation study on cross section measurement of neutrino interaction with Fe and Pb. The motivation is to give an

estimate of the achievable limit in the experiment of neutrino cross section measurement with a segmented detector at Spallation Neutron Source(SNS).

At SNS, protons are driven to hit a target, producing a large amount of neutrons and by-product pions. The negative pions are mostly captured in the target, while the positive pions, after having been stopped in the target within 0.1 ns or so, undergo the characteristic successive decay scheme  $\pi^+ \xrightarrow{26 \text{ ns}} \mu^+ + \nu_\mu$  and followed by  $\mu^+ \xrightarrow{2200 \text{ ns}} e^+ + \nu_e + \bar{\nu}_\mu$ . The resultant  $\nu_e$ 's can have a flux up to  $2 \times 10^7$  /cm<sup>2</sup>/s at a distance of 20 meters away from the spallation target for the SNS at the Oak Ridge National Laboratory, assuming the SNS power to be 1 MW [7]. Since the time structure of SNS beam provides a unique advantage for neutrino studies[7, 10, 11], backgrounds are strongly suppressed. In the SNS target, the pions are stopped and decay to muons. The subsequent muon decay produces equal intensity of  $\nu_e$  and  $\bar{\nu}_\mu$ , with a maximum energy 52.8 MeV. The energy spectra of the three kinds of neutrinos are shown in Fig.1.

Such an energy range overlaps extremely well with

that of supernova neutrinos. This characteristics makes it valuable to measure cross sections of interactions between neutrinos and various target materials at SNS. Fig. 2 shows the sketch of neutrino detector at SNS. A  $\nu$ -SNS project[7] was proposed to build a neutrino facility at the SNS at Oak Ridge National Laboratory. However, there is no report on how precise the measurement can be achieved.

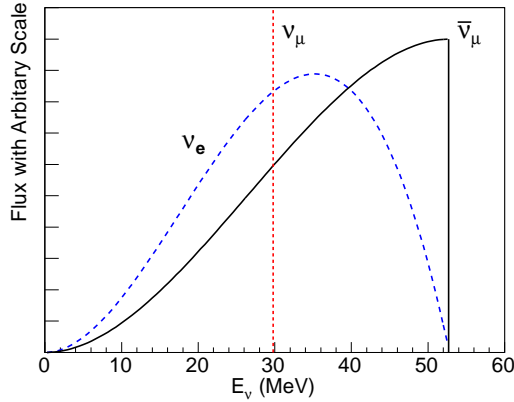


Fig. 1. Neutrino spectrum from muon and pion decay-at-rest at a spallation neutron source.

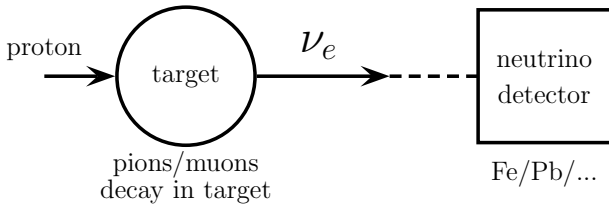


Fig. 2. Sketch of neutrino detector at SNS.

Electron neutrinos interacting with target material at the SNS undergo both neutral- and charged-current interactions, while muon neutrinos can only undergo neutral-current interactions due to the limitation of kinematics. The neutral-current events are suppressed by at least two orders of magnitude in comparison with the charged-current events and can only be measured by the decay of excited nucleus. The charged-current events can be detected via the outgoing electron in the neutrino-nucleus reaction  $\nu_e + {}^A_Z X_N \rightarrow {}^A_{Z+1} Y_{N-1} + e^-$  ( $\nu_e + n \rightarrow p + e^-$ ). Since the neutrino energy is much lower than the nucleus, considering the charged-current quasi-elastic(CCQE) process and ignoring fermi motion of nucleus, the neutrino energy  $E_{\nu_e}$  can be determined by the induced electron energy  $E_e$ ,

$$E_{\nu_e} = E_e + \Delta, \quad (1)$$

where  $\Delta$  is the mass difference between the final state nucleus Y and the initial state nucleus X. There-

fore, a precise energy reconstruction of the  $\nu_e$  induced electrons is essential to determine the differential cross sections. The segmented detector is proposed to measure the trajectories of  $\nu_e$  induced electrons in the target. However, the energy loss of the electron is dominated by ionization at low energy, while above the critical energy  $E_c$ , it will be dominated by bremsstrahlung. The electromagnetic shower caused by bremsstrahlung will lead to large uncertainty on the measurement of electron track length for energy above  $E_c$ . The critical energy can be approximated [8, 9] by  $E_c = 800 \text{ MeV}/(Z + 1.2)$ , where  $Z$  is the atomic number of the target nucleus. Therefore the critical energy of Fe is  $E_c = 29.4 \text{ MeV}$ , and  $E_c = 9.6 \text{ MeV}$  for Pb. This makes it impossible to obtain the electron energy by its track length event by event. In this paper, we will show a statistical application to unfold the distorted energy spectrum, and leading to a reasonable resolution of the differential cross section.

The outline of this paper is as followed. In section 2, the Geant4 simulation of neutrino induced electrons are simulated in Fe and Pb. The simulation results and analysis are described in section 3, and a brief conclusion is made in section 4.

## 2 Simulation procedure

To simplify the issue, we use a cube block target material with a fiducial volume of  $1 \times 1 \times 1 \text{ m}^3$ , in stead of the segmented detector with target, tube, wire, etc. The tracking resolution is assumed to be perfect. Geant4 (version 9.0p01) package [12] is applied in this simulation study.

The cross section of neutrino-nucleus scattering is rather small, we therefore directly simulate the behaviors of the induced electron in the target. The input energy spectrum of electron is the Michel distribution shaped by the theoretically predicted cross section given by R. Lazauskas and C. Volpe [4]. The maximum energy of induced electron,  $E_{\text{max}}$ , is approximately 48.2 MeV on  ${}^{56}\text{Fe}$ , and the threshold energy of the interaction is  $E_{\text{thres}} \simeq 5.1 \text{ MeV}$ . For  ${}^{208}\text{Pb}$ ,  $E_{\text{max}} \simeq 49.9 \text{ MeV}$ , and  $E_{\text{thres}} \simeq 3.4 \text{ MeV}$ .

Daughter products e.g.,  ${}^{56}\text{Co}$ ,  ${}^{208}\text{Bi}$  are ignored, since the life times of the daughters are long comparing the search window ( $\sim 10$  micro seconds).

The material of the detector is selected to be iron or lead with natural abundances, but not pure  ${}^{56}\text{Fe}$  or  ${}^{208}\text{Pb}$ . Therefore, the measured cross section is an average of mixture isotopes of iron or lead. This affects iron little since the natural abundance of  ${}^{56}\text{Fe}$  is

91.754%. For lead, the natural abundances of  $^{208}\text{Pb}$ ,  $^{207}\text{Pb}$  and  $^{206}\text{Pb}$  are 52.4%, 22.1% and 24.1% respectively, the effect of the mixture should be considered seriously in later studies.

For the interaction of electrons in nuclear material, electromagnetic process is the most important one. The processes of multiple scattering, low energy ionization and low energy bremsstrahlung are added for electrons in the simulation.

To perform the unfolding procedure [13–15], two kinds of spectra of electrons are generated: 1) Michel distribution used to obtain the detector response matrix; 2) Michel distribution weighted with the cross section of corresponding  $\nu_e$ -nucleus interaction. The second one is considered as the true distribution to be reconstructed. For each event, the electron's energy (input)  $E$  and track length  $L$  in the target are recorded.

The number of events attainable in one nominal year (assuming  $10^7$  seconds) is estimated by considering the flux of electron neutrino, the size of detector and the average cross section of  $\nu_e$ -nucleus scattering. The expected maximum cross section at 52.8 MeV for Fe is  $\sigma_{\text{Fe,max}} \simeq 1.2 \times 10^{-39} \text{ cm}^2$ , and it gives that the average cross section over energy is about  $0.3\sigma_{\text{Fe,max}}$ . For Pb,  $\sigma_{\text{Pb,max}} \simeq 1.3 \times 10^{-38} \text{ cm}^2$ , and the average cross section over energy is about  $0.4\sigma_{\text{Pb,max}}$ . Assuming the effective volume of target is  $1 \text{ m}^3$ , and the flux of  $\nu_e$ 's is  $2 \times 10^7 \text{ cm}^{-2}\text{s}^{-1}$ , the number of events in one nominal year is estimated to be  $6.1 \times 10^3$  for Fe target, and  $3.4 \times 10^4$  for Pb target.

### 3 Unfolding method

In the energy measurement, due to detector resolution, efficiency and sometimes intrinsic physical reason, the true value in bin  $i$ , will usually migrate into measured energy bin  $j$ . In other words, the measured distribution is usually distorted by the detector response, or the detector response is folded to the true distribution, leading to the measured distribution. In many cases, the true distribution could be restored by applying correction factors to the measured distribution. This method fails, however, if the relation between true value and measured ones is highly non-linear where the behavior of detector response is poor.

Suppose the true distribution is  $X_{\text{true}}$ , and the measured one is  $Y_{\text{obs}}$ . If effects of efficiency and background are ignored, they satisfy

$$Y_{\text{obs}} = R \cdot X_{\text{true}}, \quad (2)$$

where  $R$  is the response matrix or the migration ma-

trix which describes the effects of detector response. The basic idea of unfolding is that the effects of detector response could be removed or unfolded by inverse of the response matrix, i.e., the estimator of the true distribution  $X$  is

$$\hat{X}_{\text{true}} = R^{-1} \cdot Y_{\text{obs}}. \quad (3)$$

However, although this is the unbiased estimator with smallest variance, the physics is totally swept out by unphysical oscillation. The regularization is needed to remove the unphysical oscillation, which is actually a compromise between bias and unphysical oscillation, controlled by the choice of regularization parameter. There are several different schemes of regularization [13–15], for example, Tikhonov regularization, regularization based on entropy, Bayesian regularization, regularization based on Singular Value Decomposition(SVD), etc. The basic point of all is that the true distribution is believed to be smooth but not oscillating rapidly. In this study, we used the TSVDUnfold class in ROOT package[18]. TSVDUnfold is a class in ROOT for unfolding based on SVD technique, it is part of RooUnfold, a ROOT unfolding framework, developed by Tim Adye, *et al* [19].

In the SNS neutrino experiment, to measure the differential cross section of neutrino-nucleus scattering, the true value is the energy of incident electron, which is principally unknown and supposed to be binned in histogram  $E$ , the measured value is the electron track length in the target, binned in histogram  $L$ . The response matrix  $R$  can be obtained by Monte Carlo simulation as long as we have full knowledge on the detector. In discrete expression,

$$L_j = \sum_{i=1}^{n_a} R_{ji} \cdot E_i \quad (j = 1, \dots, n_b), \quad (4)$$

where  $E_i$  is number of events in bin  $i$  of  $E$ ,  $L_j$  is number of events in bin  $j$ ,  $n_a$  and  $n_b$  are numbers of bins of  $E$  and  $L$  respectively. The physical meaning of  $R_{ji}$  is the probability of an event in bin  $i$  of true distribution to migrate into bin  $j$  of measured distribution. Therefore, the response matrix is actually the normalized two-dimensional scattering plot of  $L$  and  $E$ .

### 4 Simulation results and analysis

In the simulation, the electron track length  $L$  is directly read from Geant4 with no uncertainty. The response matrix of detector with the iron target is shown in Fig. 3(a), and that of detector with the

lead target is shown in Fig. 3(b), corresponding to 200,000 electrons with Michel distributed energy. If the matrix were diagonal, one can easily obtain the energy of incident electron through track length event by event. However, these two plots show significant non-diagonal elements of the response matrices, and hence it is impossible to obtain directly the incident

energy through track length. Especially, it is obvious that the track length in iron target is smeared widely with energy above 30 MeV, while for lead target the smearing begins with energy above 10 MeV or so. This is the consequence of electromagnetic shower. Both simulations are exactly consistent with the expected critical energies of Fe and Pb.

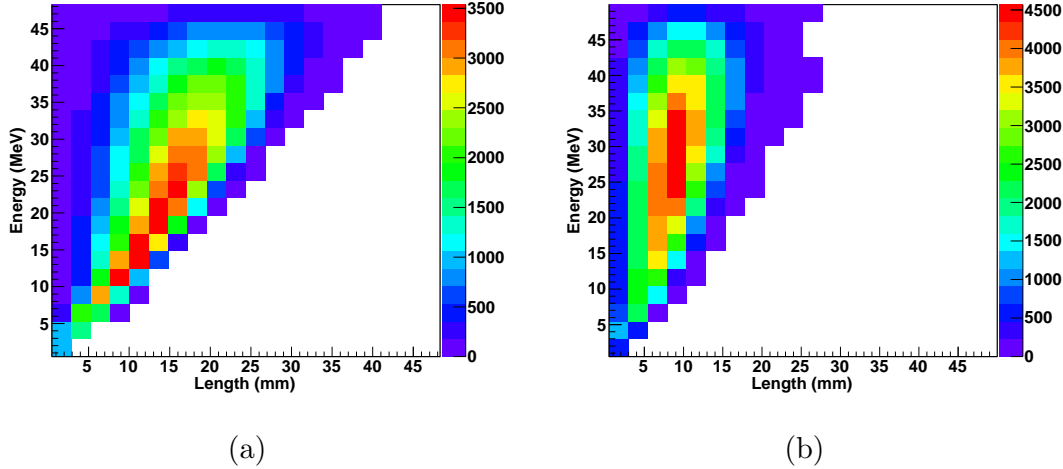


Fig. 3. Scattering plot of electron energy  $E$  versus track length  $L$  for target of Fe (a) and Pb (b). Significant non-diagonal elements of response matrix exist due to electromagnetic shower above critical energy  $E_c$ . The energy spectrum of incident electrons is Michel distribution.

To extract the physical part out of the unphysical oscillation, the choice of regularization parameter is crucial, which reflects a trade-off between bias and oscillation. For the unfolding based on the SVD technique, the choice of regularization parameter should be tuned for given distribution, number of bins and sample size. As described in Ref. [17], the regularization parameter  $kterm$  should be chosen by the plot of  $\log|d|_i$  versus  $i$ , where integer  $i$  is from 1 to the number of bins and the  $i$ th component of the vector  $d$  is the coefficient in the decomposition of the measured (and re-scaled) histogram. Only the first few terms, say  $k$ , of the decomposition should be significant for a reasonably smooth measured distribution, while the others correspond to contribution of quickly oscillating basis vectors, and should be compatible with zero. Therefore, one should see two separate patterns on the plot of  $\log|d|_i$ : for small  $i$ ,  $|d_i|$  is significantly greater than 1 and falls gradually to a standard gaussian distribution for large  $i$ . One should choose the regularization parameter  $kterm$  to be the critical value  $i = k$ , after which  $d_i$ 's are insignificant.

Fig. 4(a) shows the plot of  $\log|d_i|$  versus  $i$  with 5,000 events accumulated in Fe target, approximate data of one nominal year. The parameter  $kterm = 5$  is chosen from this plot. The unfolded energy spectrum of the  $\nu_e$  induced electron is shown in the upper

plot of Fig. 5(a), while the lower plot shows the discrepancy between the unfolded spectrum and the true one, where the latter is Michel distribution shaped by theoretical prediction of differential cross section. With the unfolded energy spectrum of the induced electron, one can obtain the spectrum of the  $\nu_e$ 's that interact with the Fe target using Eq. (1). Dividing this spectrum by Michel distribution gives the differential cross section of  $\nu_e$ -nucleus scattering, as shown in the upper plot of Fig. 6(a). The lower plot in Fig. 6(a) shows the relative discrepancy between the measured cross section and the true one. One can see that the discrepancies and errors are huge for energy below 20 MeV, mainly because the cross section of low energy is too small and few events are collected in this range. The discrepancy of the last bin is also large, around 30%. For other bins, the discrepancies are controlled within 20%. We checked this result by comparison with five other samples under the same condition. It shows that for energy below 20 MeV the measured cross sections fluctuate significantly, therefore totally unreliable. While the discrepancies between 20 and 50 MeV are well controlled within 20%. Increasing the sample size to be 10000 slightly improves the behavior between 20 and 50 MeV, but helps less(if not nothing) to the region below 20 MeV.

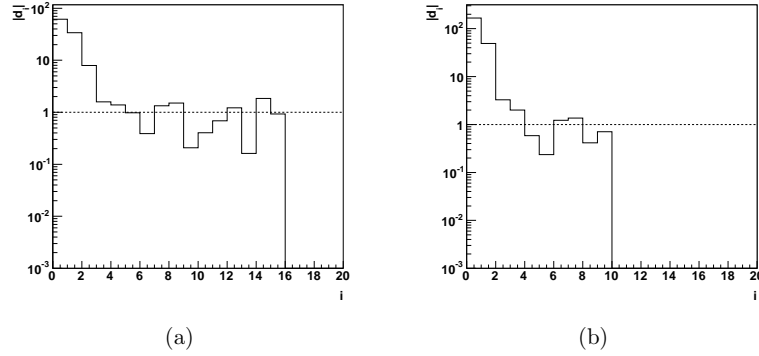


Fig. 4. Plots of  $\log|d_i|$  versus  $i$  for target of Fe (a) and Pb (b). The number of bins is 20 for both targets, while the number of measured events is 5,000 for Fe and 30,000 for Pb.

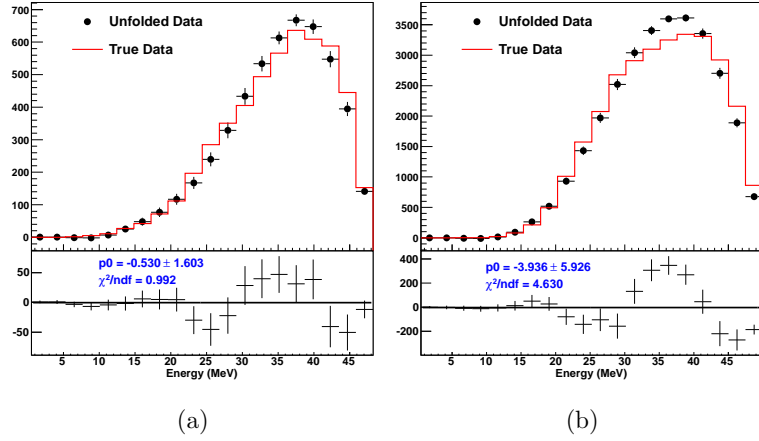


Fig. 5. Comparison between the unfolded and true energy spectra of the  $\nu_e$  induced electrons, The target is Fe for (a) and Pb for (b). The number of bins is 20 for both targets, while the number of measured events is 5,000 for Fe and 30,000 for Pb.

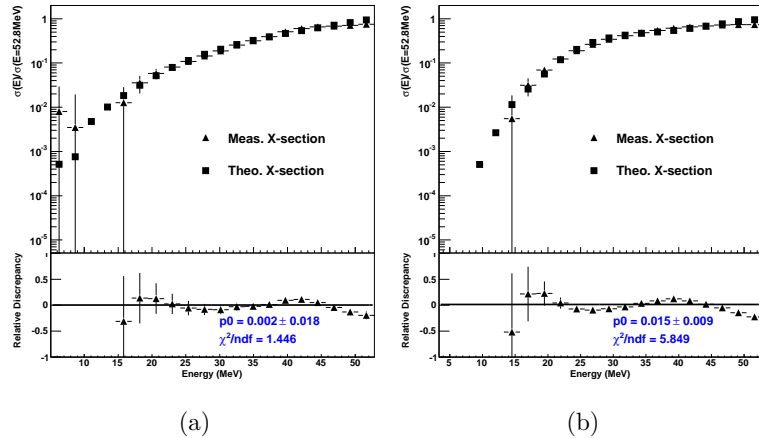


Fig. 6. Comparison between the measured and true differential cross sections of  $\nu_e$ -Fe (a) and  $\nu_e$ -Pb (b) scattering. The number of bins is 20 for both targets, while the number of measured events is 5,000 for Fe and 30,000 for Pb.  $\sigma(E=52.8\text{MeV})$  is  $1.2 \times 10^{-39}\text{cm}^2$  for Fe and  $1.3 \times 10^{-38}\text{cm}^2$  for Pb.

For Pb target, the sample size is 30,000. Fig. 4(b) shows the plot of  $\log|d_i|$  versus  $i$ , according to which, the regularization parameter  $kterm=4$  is chosen for Pb. The unfolded energy spectrum of the  $\nu_e$  induced

electron is shown in the upper plot of Fig. 5(b), and the lower plot shows the discrepancy between the unfolded and true spectrum, where the true one is Michel distribution shaped by theoretically predicted

cross section of  $\nu_e$ -Pb interaction. The resulting differential cross section of  $\nu_e$ -Pb scattering is shown in the upper plot of Fig. 6(b), and the lower plot shows the relative discrepancy between the measured differential cross section and the true one. Similar to the case of Fe target, one can see that the discrepancies and errors are large for energy below 22 MeV due to lack of events. The discrepancy of the last bin is also large, around 30%. For other bins, energy between 25 and 50 MeV, the discrepancies are well controlled within 20%. This result is compared with five other samples using the same regularization parameter. It shows that for energy below 22 MeV the measured cross sections fluctuate significantly, therefore totally unreliable. While the discrepancies between 22 and 50 MeV are well controlled below 20%.

## 5 Conclusions

With Monte Carlo simulation, we studied the achievable accuracy for the  $\nu_e$ -nucleus scattering cross

section measurement using an ideal segmented detector. Two different target materials, Fe and Pb, are investigated, since they are most relevant to the evolution of supernova and experimental data of the cross section are still not available. The energy spectrum of the  $\nu_e$  induced electron can be well reconstructed using the unfolding method, therefore makes it feasible for the measurement of differential cross section. For Fe target, the cross sections between 20 and 50 MeV can be measured within 20% accuracy using 5,000 events, the cross sections below 20 MeV is however totally unreliable since the cross section is too small in this region. For Pb target, the cross sections between 22 and 50 MeV can be measured within 20% accuracy using 30,000 events, the cross sections below 22 MeV are not reliable due to low statistics.

*We are grateful for the fruitful discussions with Dr. X. Zhu and Dr. Y. Lin for helpful discussions. This work is partly supported by the National Natural Science Foundation of China under contract number 10875062.*

## References

- 1 BETHE H A. Rev. Mod. Phys., 1990, **62**: 801—866.
- 2 TOTANI T, SATO K. Astropart. Phys., 1995, **3**: 367—376.
- 3 KUZMIN K S, LYUBUSHKIN V V, NAUMOV V A. Eur. Phys. J. C, 2008, **54**: 517—538
- 4 LAZAUSKAS R, VOLPE C, Nucl. Phys. A, 2007, **792**: 219—228
- 5 BODMANN B et al(KARMEN collaboration). Phys. Lett. B, 1992, **280**: 198—203
- 6 AUERBACH L B et al(LSND collaboration). Phys. Rev. C, 2001, **64**: 065501
- 7 Physics Division of the Oak Ridge National Laboratory. Proposal for a Neutrino Facility at the Spallation Neutron Source. 2005
- 8 BERGER M J, SELTZER S M. Tables of Energy Losses and Ranges of Electrons and Positrons, NASA-SP-3012, Washington DC, 1964.
- 9 NAKAMURA K et al(Particle Data Group). J. Phys. G, 2010, **37**: 075021
- 10 MASCHUW R(for the KARMEN collaboration). Prog. Part. Nucl. Phys., 1998, **40**: 183—192
- 11 ARMBRUSTER B et al(KARMEN Collaboration). Phys. Lett. B, 1998, **423**: 15—20
- 12 <http://geant4.cern.ch>
- 13 COWAN G. Statistical Data Analysis. Oxford: Clarendon Press, 1998.
- 14 ALBERT J et al(MAGIC collaboration). Nucl. Instr. Meth. A, 2007, **583**: 494—506
- 15 ANYKEEV V B, SPIRIDONOV A A, ZHIGUNOV V P. Nucl. Instr. Meth. A, 1991, **303**: 350—369.
- 16 FRIEDMAN J H. Data Analysis Techniques for High-Energy Particle Physics, Lectures presented at CERN School of Computing. Godoyssund, Norway, Aug11-24, 1974.
- 17 HÖCKER A, KARTVELISHVILI V. Nucl. Instr. Meth. A, 1996, **372**: 469—481
- 18 <http://root.cern.ch>
- 19 <http://hepunix.rl.ac.uk/~adye/software/unfold/RooUnfold.html>